Copper Nanoparticle-Coated Fabrics for Rapid and Sustained Antibacterial Activity Applications

Rui A. Gonçalves‡§, Joanne W. K. Ku‡$, Hao Zhang§, Teddy Salim#, Guodong Oo$, Alfred A. Zinn%, Chris Boothroyd#, Richard M. Y. Tang$, Chee Lip Gan§*, Yunn-Hwen Gan$, Yeng Ming Lam§**

‡These authors contributed equally.

§School of Materials Science and Engineering, Nanyang Technological University, 50 Nanyang Avenue, Singapore 639798, Singapore. E-mail: clgan@ntu.edu.sg; E-mail: ymlam@ntu.edu.sg

School of Materials Science and Engineering and Facility for Analysis Characterisation Testing and Simulation, Nanyang Technological University, 50 Nanyang Avenue, Singapore 639798, Singapore

$ Infectious Diseases Translational Research Program, Department of Biochemistry, Yong Loo Lin School of Medicine, National University of Singapore, MD 7, 8 Medical Drive, Singapore 117596, Singapore. E-mail: bchganyh@nus.edu.sg

% Kuprion, Inc., 4425 Fortran Dr., San Jose, CA 95134, USA

KEYWORDS: copper, nanoparticles, antibacterial, coatings, oxidative stress, DNA fragmentation.

ABSTRACT

The scientific community has recognized that copper can kill bacteria; however, the effect of particle size, concentration, and oxidation state on antibacterial activity remains unclear for copper and its nanoparticles, in particular. In this study, copper nanoparticle coatings with extremely fast and sustained antibacterial activity are reported. It is found that coating with cuprous oxide (Cu_2O) nanoparticles (~150 nm), and coating with metallic copper nanoparticles (~50 nm) on commonly used fabrics for cleaning and masks can kill bacteria within 45 seconds. Our bacterial study was conducted using *Staphylococcus aureus* as a Gram-positive bacterium, and *Klebsiella pneumoniae* and *Pseudomonas aeruginosa* as Gram-negative bacteria. Scanning electron micrographs suggest bacterial damage, and bacterial DNA harvested after interaction with copper-coated fabrics indicate DNA fragmentation. On top of this, significantly higher levels of 8-oxo-2'-deoxyguanosine are also detected in DNA after interaction with coated fabrics, signifying that both copper and Cu_2O nanoparticles rapidly induce oxidative stress. Furthermore, cumulative inoculations with *K. pneumoniae* for 144 hours show excellent sustained bacterial killing in the presence of Cu_2O nanoparticles. Using a combination of detailed physical and chemical analysis of the nanoparticles and study of how bacteria interact with the coated substrate, it is possible to establish the parameters that resulted in speedy and robust antibacterial properties in Cu_2O-coated fabrics. This study offers a rational strategy on how to slow down or even halt the transmission of infectious pathogens.

INTRODUCTION

The pandemic caused by the SARS-CoV-2 virus has been partly due to the ease of transmission of this virus amongst humans. This created a great urgency to impart surfaces with antiviral and

antibacterial agents as an attempt to slow down or even halt the transmission of infectious pathogens and their diseases via high touch surfaces. Transition and noble metals, in various forms such as bulk material, nanoparticle and surface coating, have been shown to be effective antibacterial agents. In 2011, the U.S. Environmental Protection Agency (EPA) approved and added 73 new copper alloys with antimicrobial activity to the list that was first published in 2008, raising the total number of EPA-approved antimicrobial copper alloys to 355.[1-2] This approval drove the development of solid copper surfaces capable of killing more than 99.9% of methicillin-resistant *Staphylococcus aureus*, an antibiotic-resistant species of Gram-positive bacteria that is a frequent source of hospital-acquired infections.[1, 3] Copper has been recognized as the first effective metallic antimicrobial agent known in history, and the shortest reported duration required for killing bacteria on wet surfaces is 30 minutes against *Clostridium difficile*,[4] and more than 60 minutes against *Escherichia coli*.[5-6] The antibacterial activity of copper through "contact-killing" is believed to be primarily due to two factors: i) the dissolution of copper ions, which can penetrate and damage the bacterial cell wall;[7-12] and ii) the cyclic redox reactions between Cu^+ and Cu^{2+}, which generates reactive hydroxyl radicals (reactive oxygen species, peroxides)[7, 9-11, 13-15] by Fenton-type (Equation 1 and 2) and Haber-Weiss reactions (Equation 3):[9-10, 15-16]

Equation 1: $Cu^{2+} + H_2O_2 \leftrightharpoons Cu^+ + \cdot HO_2 + H^+$

Equation 2: $Cu^+ + H_2O_2 \rightarrow Cu^{2+} + \cdot OH + OH^-$

Equation 3: $O_2^- + H_2O_2 \rightarrow O_2 + \cdot OH + OH^-$

Furthermore, a study done on *Escherichia coli* as the surrogate bacterial species suggested that the copper-mediated inactivation results from the interaction between the released ionic species (Cu^+ or Cu^{2+}) and the cell components, with the cuprous species (Cu^+) exhibiting better toxicity under

anaerobic conditions.[17] Even when a "dry" inoculum protocol was employed, *E. coli* could still be effectively killed by copper surfaces within 30 min owing to the combination of reactive oxygen ions and radicals, which leads to the cytoplasmic membrane and degradation of genomic DNA.[18] Studies on copper bulk surfaces also demonstrated that cuprous oxide (Cu_2O) efficiently inactivates the influenza A virus and *E. coli* bacteriophage, and cupric oxide (CuO) was less efficient for the same exposure time, indicating that the oxidation state of copper could play an essential role in the efficacy of the biocidal surface.[14, 19] Although the antibacterial properties of solid copper surfaces have been the subject of intensive research, the "contact-killing" mechanisms associated with copper nanoparticles (NPs) remain controversial.[9, 11, 20] Furthermore, the reports on the fastest antibacterial activity of copper were performed using the dry method[21-22], which did not allow for inferences to be made against pathogen-loaded droplets.[23] For the coating of soft compliant surfaces, a bulk solid coating is less useful, and it will change the mechanical behavior of the base materials, hence other forms of materials have to be considered.

Nanoparticles have a high surface-area-to-volume ratio that makes them highly reactive. Therefore, they are good potential candidates to endow surfaces with higher antibacterial activity as compared to solid bulk copper surfaces. Recently, researchers have investigated the stress-induced rupture of the bacterial cell membrane, especially for large non-translocating NPs. They demonstrated that the adsorption of gold NPs on the surface of bacteria increases the membrane tension, hence causing membrane deformation and rupture.[20, 24-26] Although there is an increasing number of published review articles on antimicrobial metal and metal oxide nanoparticles[27-31], highlighting the growing importance of the family of materials within the field, the mechanistic understanding of the roles of metallic copper or copper NPs as an antibacterial agent remains elusive. For example, in their attempt to shed some light on the antibacterial efficacy of copper

oxide NPs, Meghana and coworkers discovered that *E. coli* was inactivated by different mechanisms: formation of Cu^{+}–peptide complex and generation of radical species for Cu_2O and CuO, respectively.[32] However, not only was the study limited to freestanding NPs in liquid, it also did not evaluate the impact of factors such as ions released into the medium, NP agglomeration and dispersion stability, surface coating and charge, pH of the medium, etc. Therefore, the elucidation of the antibacterial (and potentially antiviral[33-36]) "contact-killing" properties of copper NPs with different oxidation states and surface charge properties, coated on the same platform and with the same deposition route, is imperative for the understanding of which form of copper particles will be effective in the prevention of the propagation of infectious agents and the reason behind it.

In order to effectively reduce the transmission of viruses and bacteria, other than imparting high touch flat and rigid surfaces with antibacterial properties, it is also necessary to impart non-rigid surfaces and surfaces with different curvatures with such properties. One such example of a non-rigid and conformal surface is fabric materials used in applications such as face masks, upholstery, etc.[37] It is important to be able to impart antibacterial properties to such flexible and breathable materials to safeguard the population against infectious pathogens. To do this, researchers have been using two strategies that are effective for fabrics. One approach is to impart the fabric with water-repelling properties, and that is to make the fabric more hydrophobic, which minimizes the wetting and hence absorption of pathogen-loaded polar medium or matter.[38] However, this approach may not stop or prevent the propagation of pathogens as the pathogens are still present on the surface and may permeate through the fabric during prolonged use. This approach will also be ineffective in high-humidity environments. The other alternative is to use a metal or metal oxide NP (with effective antibacterial properties) coating on the fabrics or surfaces of interest. This

method would allow the inorganic components in the coatings, such as copper-based components, to come in contact with the pathogens and effectively "kill" the bacteria via one of the "contact-killing" mechanisms which we have discussed previously, hence creating robust and highly active biocidal surfaces.

In this paper, we set out to elucidate the impact of concentration, nanoparticle size, surface charge properties and the oxidation state of copper-based compounds on clinical isolates of multi-drug resistant bacteria in droplet form on fabric surfaces to approximate real-life scenarios in an urban environment. This is one of the first few systematic studies to unravel the chemical/structural-activity relationship of copper nanoparticles. This will contribute towards the design of an effective antibacterial formulation that makes use of a combination of parameters that can result in a rapid "contact-killing" effect. There are two crucial but often neglected characteristics to evaluate the effectiveness of antibacterial coatings for practical application: (1) the time taken for killing to happen and (2) whether this killing is sustained or just ~~a~~ one-off. We show that with the right combination of material properties, it is possible to obtain a robust copper NP-coated fabric capable of readily inactivating infectious agents (within 45 s), and the fabric can be used repeatedly with sustained effectiveness. This paves the way for a robust and effective antibacterial material that can be coated on most surfaces.

EXPERIMENTAL SECTION

Chemicals and fabrics. yCu was purchased from Chongqing Yumeco Import & Export Co., Ltd. (China). aCu was supplied by Kuprion, Inc. (USA). A commercial plastic (Scotch-Weld) adhesive was purchased from 3M (USA). Acetone and isopropyl alcohol (IPA) were purchased from Aik Moh (Singapore). These compounds were used as received. Fabric #1 was a 55/45%

cellulose/polyester fabric blend, Fabric #2 was a 70/30% rayon/polyester fabric blend, and Fabric #3 was a glossy vinyl sheet (AIVA) kindly supplied by Kuprion. aCu (1% w/w) was dispersed in IPA and sonicated in an ultrasonic bath for 2 minutes. The same method was employed for the yCu powder. The scotch-weld adhesive (2.5% w/w) was dissolved in a mixture of acetone and IPA at a 1:4.5 weight ratio.

Spray coating. Fabrics cut into squares with an area of 930 cm^2 were spray-coated with the copper dispersions and the adhesive solution using a 3M Accuspray^{TM} spray gun and dried with a heat gun. The layer of adhesive was sprayed last to prevent the loss of nanoparticles, and more importantly to impede the inhalation of airborne particulate matter.

Nanoparticle and fabric characterization. The yCu and aCu nanoparticles, in both pristine particle form and particle-functionalized fabrics, were characterized with a field-emission scanning electron microscope (SEM) (JEOL 7800F Prime) with an energy-dispersive X-ray spectroscopy (EDS) detector (Ultim Max, Oxford Instruments). The accelerating voltages used for SEM imaging and EDS analysis were 5 kV and 20 kV, respectively. To minimize the effects of charging, the non-conductive fabrics were first coated with an ultrathin layer of Pt. The X-ray photoelectron spectroscopy (XPS) spectra were collected using a Kratos AXIS Supra (Al Kα source, 225 W) over an analysis area of 700 µm x 300 µm with a take-off angle of 90°. The energy-loss spectra were recorded on a JEOL 2100F transmission electron microscope (TEM) with an accelerating voltage of 200 kV and a Gatan imaging filter. The Auger Electron Spectroscopy (AES) measurements were conducted on a JEOL JAMP-7830F machine equipped with a field-emission electron gun and a hemispherical analyzer. The AES analysis was performed at an acceleration voltage of 10 keV and a probe current of 10×10^{-9} A. The sample was tilted at 30° throughout the analysis and the analysis area was approximately 15 x 15 μm^2. The zeta potential

of the copper nanoparticles dispersed in deionized water with a concentration of 0.01% (w/v) was determined using a Zetasizer (Malvern Instruments). The pH values of the water dispersions of yCu or aCu were adjusted from 5 to 11 using dropwise addition of either 0.05 M hydrochloric acid or 0.05 M sodium hydroxide.

Bacterial strains. The bacterial strains used in this study include carbapenem resistant hypervirulent *Klebsiella pneumoniae* ENT646[39], laboratory stock strain *Pseudomonas aeruginosa* PAO1, and *Staphylococcus aureus* ATCC strain SA29213. Bacterial strains were routinely cultured and maintained on lysogeny broth (LB) agar.

Preparation and treatment of fabrics with bacteria. Circular discs of 6 mm diameter were prepared with a 6 mm hole punch and sterilized via ultraviolet (UV) exposure for at least an hour. Fabric samples were pre-wet with 5 µL of sterile deionized H_2O before inoculation with 5 µL of bacterial cultures at various doses for a defined contact time.

Determination of antibacterial activity. After inoculation of bacterial cultures onto the fabrics for the indicated duration, the fabrics were clipped to the lid of an Eppendorf tube and centrifuged at maximum speed for 1 minute, retrieving the liquid absorbed by the fabrics. The fabrics were then washed in sterile phosphate-buffered saline (PBS; Vivantis) to retrieve adherent bacteria, if any. The resultant solution from the fabrics and wash solutions were serially diluted and plated on LB agar and incubated at 37 °C overnight. Percentage killing was calculated by comparing bacterial numbers obtained from fabrics with yCu or aCu to the average bacterial counts obtained from control fabrics F#1, F#2 or F#3, according to the formula: 100 - (counts from the fabric of interest/average counts from control * 100). For experiments with repeated inoculation of bacteria, 10^4 CFU of *Klebsiella pneumoniae* ENT646 were inoculated sequentially, as described above,

thrice a day for five consecutive days at 0, 3, 7, 24, 27, 31, 48, 51, 55, 72, 75, 79, 96, 99, 103 hours and on day 7, at 144 hours. At each timepoint, bacteria were retrieved from fabrics for the determination of bacterial numbers and percentage killing as described above. Fabrics were inoculated with 10^8 CFU of *Klebsiella pneumoniae* ENT646 for 1 hour to image the interaction of the bacteria with the NP-coated fabrics. Fabrics were then fixed in 4% paraformaldehyde for 15 minutes and washed in 10 mM glycine twice before three washes in deionized H_2O. Fabrics were then dried overnight in a desiccator cabinet and imaged with the SEM.

Examining DNA fragmentation. Bacterial genomic DNA extraction was performed according to Weaver *et al*.'s methodology[40], with minor modifications. Briefly, five fabric samples were inoculated with 10^8 CFU of *K. pneumoniae* ENT646. After 45 seconds or 1 hour at room temperature, fabrics were transferred to sterile PBS with 20 $mmol^{-1}$ EDTA and vortexed for 30 seconds. Bacterial cells were pelleted by centrifugation at 4000g for 5 minutes. Bacterial genomic DNA was isolated and purified with GenElute™ Bacterial Genomic DNA kit (Sigma). Isolated DNA was examined via gel electrophoresis.

Oxidative DNA damage analysis. To examine the amount of oxidative damage in DNA, the fabric was pre-wet with 10 mM Tris-HCl buffer pH 8.0 before the addition of 50 µg of deoxyribonucleic acid (DNA; Sigma). After 45 seconds or 1 hour, fabrics were clipped to the lid of an Eppendorf tube and centrifuged at maximum speed for 1 minute. DNA retrieved was hydrolyzed and examined via LC-MS for levels of 8-hydroxy-2' -deoxyguanosine (8OHdG).

Statistical Methods. Statistical significance of 95% confidence between three or more groups were determined by ANOVA followed by Tukey's test. All statistics were conducted using the

GraphPad Prism software. Statistical significance is indicated as follows: *P ≤ 0.05; **P ≤ 0.01; ***P ≤ 0.001.

RESULTS AND DISCUSSION

Herein, the focus of this work is to understand how the different properties of copper nanoparticles impact the effectiveness of copper nanoparticle formulations as antibacterial coatings on fabrics used for various applications. The systematic coating and characterization of the copper NP-coated fabrics is depicted schematically in Scheme 1. The copper NPs were characterized before and after spray coated on the fabrics. Their antibacterial activities, morphological effect on the bacteria, the amount of oxidative damage produced and bacterial genomic DNA fragmentation after bacterial interaction were evaluated.

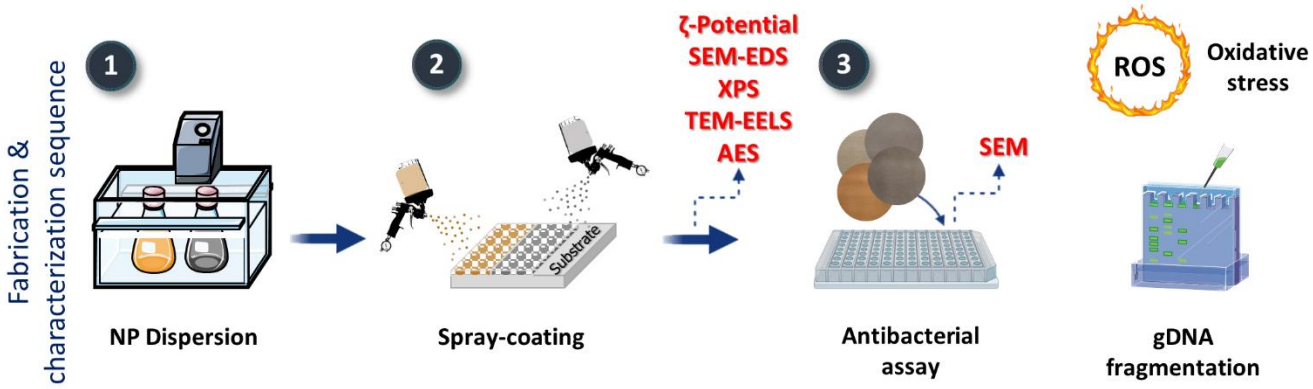

Scheme 1. The fabrication route and characterization of the copper coatings. The chemical and structural properties of copper nanoparticles were characterized using zeta-potential, SEM-EDS, XPS, TEM-EELS and AES. The nanoparticles were dispersed with the aid of an ultrasonic bath, followed by spray-coating on the substrates. Subsequently, the copper-coated fabrics were inoculated with Gram-positive and Gram-negative bacteria and SEM images were collected. The

amount of oxidative damage and bacterial genomic DNA fragmentation after bacterial interaction was assessed.

Two species of copper were used, a commercial cuprous oxide (Cu_2O), henceforth named yCu, and commercial metallic copper NPs, henceforth named aCu. Both formulations were spray-coated on two types of fabric materials commonly used to fabricate facemasks and filters in air purification units (Figure SI1) that are present in many different systems such as heating, ventilation, and air conditioning systems in hospitals and airplanes.

Copper Nanoparticles Characterization and Distribution on Substrates. Well dispersed NPs exhibit very high surface-area-to-volume ratios, which is highly advantageous in applications that require direct contact between the NPs and the pathogens. As discussed earlier, oxidation state of copper species is one important parameter that may have a significant impact on antibacterial activity.[7, 9-11, 13-15] Hence, it is important to elucidate the states of the copper NPs before and after coating onto the various fabrics to understand how this ~~property~~ and other physical properties can be manipulated to improve the antibacterial behavior of the coating. The size, shape, oxidation state, and surface charge of the copper NPs were first determined (Figure 1), and the analysis results are tabulated (Table 1). The scanning electron microscopy (SEM) image of the yCu NPs reveals hierarchical structures (Figure 1a). Small NPs with an average size of about 150 nm were observed to form large aggregates. On the other hand, aCu NPs show a smaller average size of about 50 nm with a regular spherical shape, and due to their high surface energy, form large aggregates or clumps (Figure 1f). The inherent small size of the nanoparticles gives rise to a higher surface-to-volume ratio, and its high surface energy fosters direct contact and interaction with the infectious agents.[7, 41] However, it should be pointed out that in our case, the nanoparticles were agglomerated into micron size aggregates (~1-15 μm). Even so, the uniform coverage as shown in

Figure 2 will ensure a very high probability for the pathogens to come into contact with the NPs. Using a combination of characterization techniques such as X-ray photoelectron spectroscopy (XPS), X-ray diffraction (XRD), Auger electron spectroscopy (AES), and transmission electron microscopy – electron energy-loss spectroscopy (TEM-EELS), the oxidation state of both copper species can be determined. The Cu 2p core-level spectra of both yCu and aCu show very similar features, i.e., doublets with spin-orbit splitting of ~ 19.8 eV, with the yCu showing additional weak satellite features (Figure 1c and h). Peak analysis was conducted for the Cu $2p_{3/2}$ component using Gaussian–Lorentzian line shapes as this will enable the differentiation of Cu species in both copper samples. For yCu, the deconvolution of the core-level Cu $2p_{3/2}$ signal yields a main peak at 932.3 eV and another small peak at 934.3 eV, corresponding to Cu_2O and $Cu(OH)_2$ phases, respectively (Figure 1c). The satellite features observed are attributed to the hydroxide phase. On the other hand, for aCu, the Cu $2p_{3/2}$ peak is at 932.5 eV (Figure 1h). The extracted XPS Cu $2p_{3/2}$ core-level binding energies are in the increasing order Cu(I) < Cu(0) < Cu(II), which is in good agreement with the literature.[42-43] From our quantitative analysis, about 80.6% of the whole yCu sample consists of Cu_2O. The residual $Cu(OH)_2$ was likely to be a metastable phase formed upon the interaction between Cu ions and the hydroxyl groups on the surface of Cu_2O particles.[44] In fact, XPS analysis of an aged yCu sample (Figure SI2) reveals that $Cu(OH)_2$ could account for as much as 91.9% of the total Cu, presumably due to significant water absorption on the oxide surface at high humidity. From this observation, it can also be inferred that yCu was likely to have high phase purity (~100%) in the absence of surface hydroxyl groups. Chemical state identification provided by Auger electron spectroscopy also agrees reasonably well with XPS and the XRD patterns (Figure SI3). The fitting of the differentiated AES spectra shows peaks at 915.1 eV for aCu corresponding to metallic Cu and at 913.1 eV and 914.3 eV for yCu, corresponding to the Cu_2O

and CuO phases, respectively. The AES spectra revealed a main phase of Cu_2O in yCu with an atomic concentration of 95.3% (Figure 1d), while aCu primarily consists of metallic Cu species (Figure 1i). The discrepancy in the composition of yCu provided by XPS and AES can be attributed to the difference in the sampling volume and depth of analysis. As Cu 2p photoelectrons and Cu LMM Auger electrons have different kinetic energies, i.e., 530–550 eV and 900–920 eV, respectively, XPS is expected to provide more surface-sensitive information from the sample. It is also worth mentioning that the intensity of the O KLL signal is stronger in yCu than in aCu, as shown in the AES survey-scan spectra (Figure SI4). Figures 1e and j show the two copper $L_{2,3}$ edges obtained from yCu and aCu, respectively, using TEM-EELS. The two principal features, the L_3 and L_2 edges, arise from the spin-orbital splitting of the 2*p* core hole and are separated by about 20 eV. The full black line in Figure 1e shows an asymmetric peak from one region of yCu and a feature marked by an arrow in the vicinity of the L_2 edge. The L_3 edge in this spectrum is located at 937.9 eV. Another EELS edge (blue dotted line, Figure 1e) collected from a nearby region of yCu shows a different profile, with the L_3 edge located at 938.0 eV. For aCu, shown in Figure 1j, the L_3 edge is located at 936.7 eV and the EELS edge shows no white lines. The decrease in white line intensity is due to a filled 3*d* shell which was previously described and discussed.[45-47] The spectral shape and the relative position of the L_3 edges in yCu and aCu allow us to further confirm the presence of Cu_2O and CuO in yCu, and metallic copper as the main constituent of aCu. The zeta potential measurements showed distinct trends for yCu and aCu. As pH is gradually increased from 5, the zeta potential of aCu nanoparticles shows a monotonic decrease in zeta potential values, and this implies that the surface was progressively becoming more negatively charged, with an isoelectric point (IEP) of less than pH 5 (Figure 1k). Conversely, yCu revealed a strongly positive surface at pH 6.7 with a zeta potential of 26.7 ± 0.4 mV and an IEP of 9.5 (Figure 1k). These

observations were consistent with those reported elsewhere.[48-49] Therefore, these results suggest that aCu NPs on fabrics are expected to possess a negatively charged surface at pH 7, whereas yCu NPs are likely to possess positively charged surfaces at the same pH. The bacterial viability will significantly decrease when they come into contact with these charged NPs.

The combination of XPS, AES, and TEM-EELS enables us to establish that yCu is mainly composed of Cu_2O (Cu^+), and in aCu, the copper exists almost exclusively in the metallic form (Cu^0). Additionally, zeta potential measurements showed that aCu is negatively charged across a broad range of pH values, and yCu is positively charged at neutral pH.

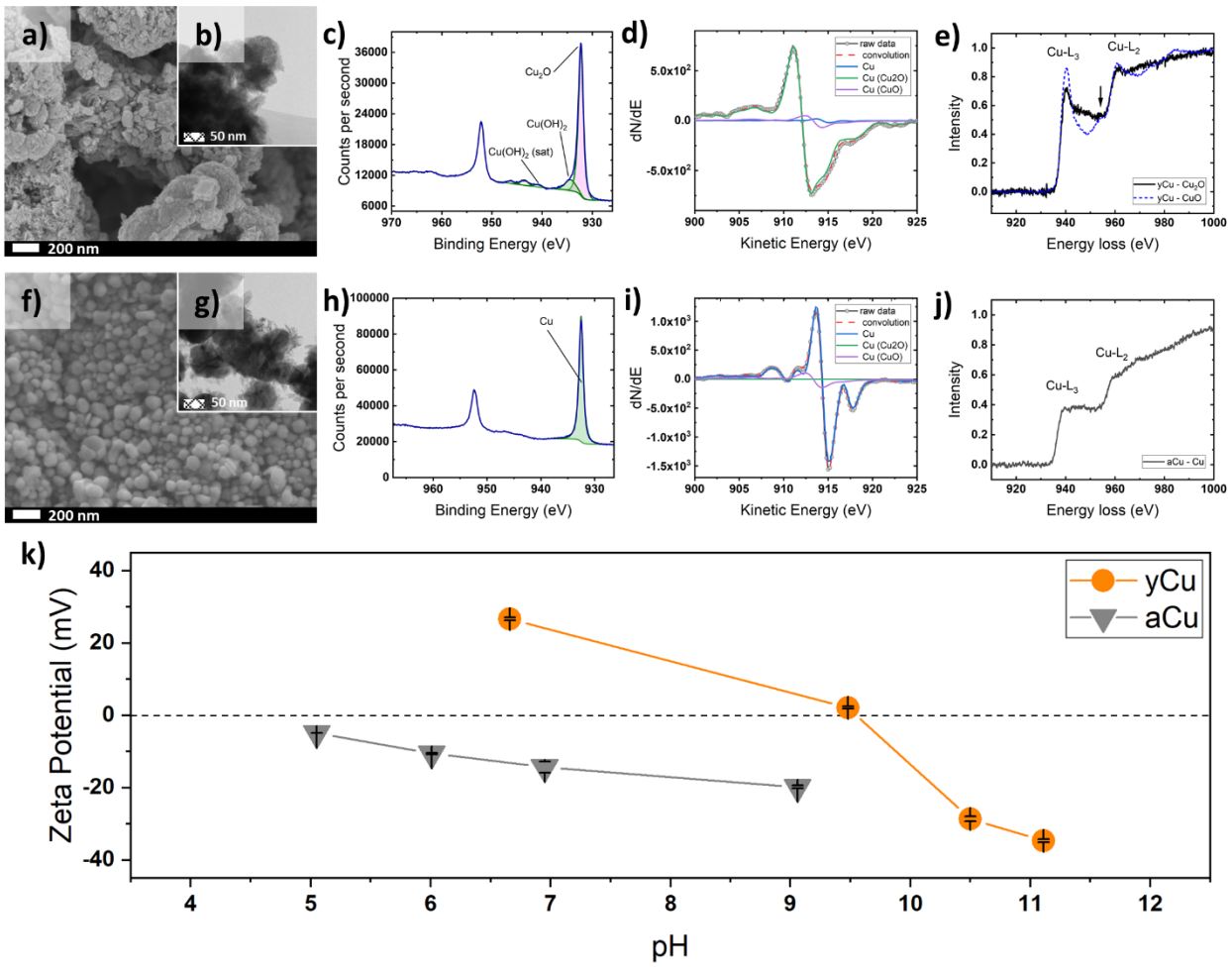

Figure 1. Characterization of the copper nanoparticles. The top row of images, (a-e), corresponds to yCu, while the bottom row, (f-j), corresponds to aCu. (a, f) SEM and (b, g) STEM images, (c, h) XPS Cu 2*p* core level spectrum, (d, i) AES Cu *LMM* spectrum, (e, j) TEM-EELS Cu $L_{2,3}$ edges. (k) Zeta potential of yCu and aCu dispersed in deionized water at various pH values.

Table 1. Cu 2p binding energies, Cu LMM kinetic energies, and Cu L_3 edge energies from the XPS, AES and TEM-EELS spectra, respectively, for the yCu and aCu nanoparticles.[50]

		XPS			
		Cu	**Cu_2O**	**CuO**	**$Cu(OH)_2$**
yCu[a]	Cu $2p_{3/2}$ binding energy [eV]	-	932.3	-	934.3
	Atomic concentration [%]	-	80.63	-	19.37
yCu[b]	Cu $2p_{3/2}$ binding energy [eV]	-	932.2	-	934.3
	Atomic concentration [%]	-	8.15	-	91.85
aCu	Cu $2p_{3/2}$ binding energy [eV]	932.5	-	-	-
	Atomic concentration [%]	100.00	-	-	-
		AES			
		Cu	**Cu_2O**	**CuO**	
yCu	Cu *LMM* kinetic energy [eV]	-	913.1	914.3	
	Atomic concentration [%]	1.0 ± 1.2	95.3 ± 5.1	3.8 ± 4.0	
aCu	Cu *LMM* kinetic energy [eV]	915.1	-	-	
	Atomic concentration [%]	88.5 ± 3.1	0.7 ± 1.6	10.8 ± 1.7	
		EELS			
		Cu	**Cu_2O**	**CuO**	
yCu	Cu L_3 edge energy [eV]	-	937.9	938.0	
aCu	Cu L_3 edge energy [eV]	936.7	-	-	

[a] Fresh sample; [b] Sample left in ambient for at least a month.

To investigate the nanoparticle distribution, SEM images and EDS maps of the copper-coated fabrics were collected at 100× and 500× magnification. The atomic concentration (at%) determined using EDS mapping does not vary significantly at different magnifications (Table SI1).

Fabric #1 (F#1) is a 55/45% cellulose/polyester fabric blend with wide and flat cellulose stripes and fabric #2 (F#2) is a 70/30% rayon/polyester fabric blend with polymer fibers sparsely distributed which may improve ~~the~~ breathability when used as the filter layer in face masks. Both yCu and aCu can be easily identified on the SEM images and are uniformly distributed in the form of large 1-15-micron size aggregates on the filter materials (refer to Figure 2). The SEM images and EDS maps collected at 100× magnification can be found in Figure SI5. The aCu appears homogeneously distributed on both fabrics, with a coverage that is approximately twice that of the yCu on fabric F#1. This can be attributed to the structure of the pristine fabrics and the size of the yCu particles. Though yCu particles are rather large, the features present on the pristine fabric F#2 (Figure 2e) facilitated the loading of yCu. On the one hand, the polymer fibers in F#2 are sparsely distributed, which contribute to enhanced airflow. A thin membrane that bridges the fibers facilitated the anchoring of NPs by providing an additional surface for particle bonding, hence contributing to a more robust coating.

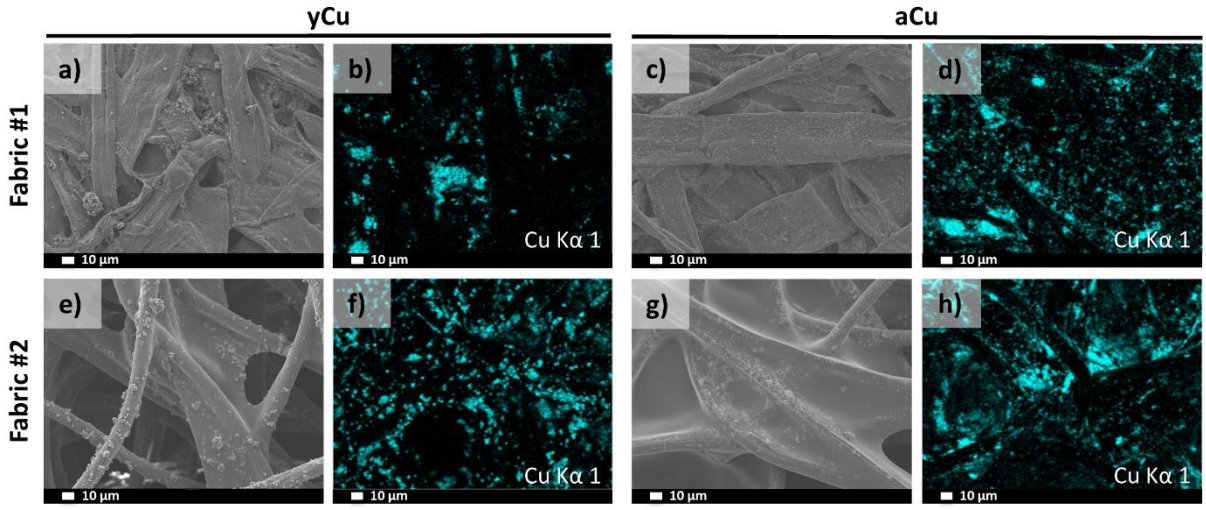

Figure 2. Distribution of the nanoparticle aggregates on the fabrics after the spray-coating process. SEM images and EDS Cu *K*α maps of yCu coated on (a-b) Fabric #1 and on (e-f) Fabric #2. SEM

images and EDS maps of aCu coated on (c-d) Fabric #1 and (g-h) Fabric #2. The scale bar is 10 µm.[50]

Influence of Copper Nanoparticles on Bacterial Killing Efficiency. To investigate the biocidal effect of the yCu and aCu NPs, the antibacterial activity of the copper-coated fabrics against Gram-negative bacteria, carbapenem-resistant cum hypervirulent *Klebsiella pneumoniae* ENT646[51] and *Pseudomonas aeruginosa* lab strain PAO1, and Gram-positive bacterium, methicillin-sensitive *Staphylococcus aureus* 29213, was investigated. Various copper-coated and their corresponding control fabrics were inoculated with 10^4 CFU bacteria for 45 seconds before the enumeration of bacterial counts. The killing efficiencies were determined by comparison of bacterial numbers obtained from the copper-coated fabrics to the average bacterial counts obtained from control fabrics F#1, F#2, or F#3. For *S. aureus*, a solid commercial vinyl film F#3 (AIVA) was used to determine biocidal effects of the NPs as the low bacterial counts retrieved from the control fabrics F#1 and F#2 (Figure SI6d) would skew killing efficiency calculations. Against all three types of bacteria, both yCu and aCu copper fabrics significantly reduced bacterial numbers as compared to control fabrics (Figure 3a-c and Figure SI7), with yCu- and aCu-coated fabrics exhibiting average killing efficiencies of >93% and >84%, respectively. No obvious difference in killing efficiencies was observed between yCu- and aCu-coated fabrics at a higher dosage of 10^5 CFU *K. pneumoniae* (Figure SI6a). However, at 10^6 CFU *K. pneumoniae*, yCu exhibited poorer killing efficiency as compared to aCu when coated on fabric F#1 whereas no difference was observed when coated on Fabric F#2 (Figure SI6b). The more efficient killing may be associated with the higher surface coverage of aCu on fabric F#1 detected from SEM-EDS, compared to yCu-coated fabric F#1 as observed in the SEM-EDS compared to yCu (Figure 2 and Table SI1). These data suggest that in

addition to the oxidation state of the copper nanoparticle, the nanoparticle concentration and the base fabric can affect the antibacterial efficacies of the copper-coated fabrics.

Further study with the NPs was performed using *K. pneumoniae* ENT646 and fabric F#1 as the base substrate. When coated on fabric F#1, yCu displayed sustained ability to kill over cumulative inoculations with 10^4 CFU *K. pneumoniae* across the duration of 144 hours while aCu-coated fabrics had a gradual fluctuating decline in killing (Figure 3d and e). This demonstrates that yCu is more robust than aCu. Notably, bacterial surface charges are mostly negative. This is due to the presence of negatively charged molecules such as teichoic acids and lipopolysaccharides in Gram-positive and Gram-negative bacterial cell walls respectively[52-53]. Negatively charged polysaccharides are also present in the bacterial capsule[54]. Regarding the bacterial strains used in this study, *P. aeruginosa* PAO1 and *S. aureus* SA29213 had been previously measured over various pH and was shown to exhibit a negative surface charge at neutral pH[55-57]. While there are no accounts of surface charge measurements for *K. pneumoniae* ENT646, the strain possesses a K1 capsule that has been previously reported to have a high content of negatively charged sialic acids[58]. As discussed earlier, the zeta potential measurements of the copper nanoparticles showed that yCu has an IEP of 9.5 while aCu has an IEP less than pH 5 (Figure 1k). Since the bacteria were inoculated onto the copper-coated fabrics at neutral pH, the positively charged yCu is expected to have stronger electrostatic interactions with the negatively charged bacteria. It is plausible that the negatively charged aCu could induce the formation of electrostatic barrier which could repel and weaken the interaction with bacteria, resulting in less robustness.

Additionally, we studied the effect of the addition of deionized water onto the copper-coated fabrics using XPS (Figure SI8) since the bacteria were dispersed in deionized water for inoculation. The water was added onto the copper-coated fabrics for 144 hours, and three data points for

analysis were selected. The addition of water onto yCu-coated fabric showed a negligible effect on the atomic concentration of $Cu(OH)_2$ present on the surface of the fabric. In contrast, the aCu-coated fabric revealed a decrease of $Cu(OH)_2$ with the exposure time (Table SI2) which could potentially account for the decline in bacterial killing over cumulative inoculation.

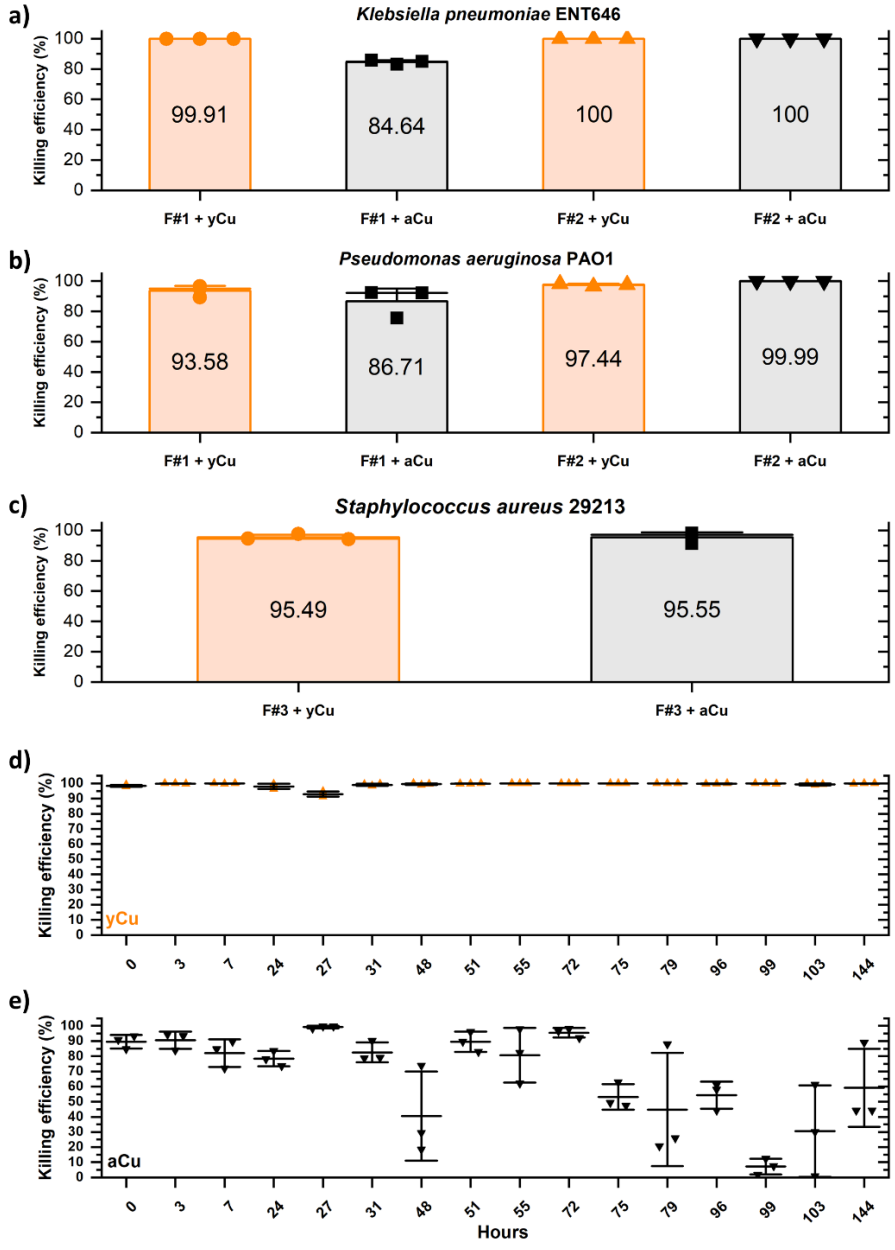

Figure 3. yCu and aCu fabrics exhibit antibacterial properties. (a-c) Killing efficiencies of various fabrics inoculated with 10^4 CFU bacteria for a duration of 45 seconds (a) carbapenem-resistant hypervirulent *Klebsiella pneumoniae* ENT646, (b) *Pseudomonas aeruginosa* PAO1 and (c) *Staphylococcus aureus* SA29213. The bacterial numbers were compared to the average bacterial counts obtained from control fabrics F#1, F#2 or F#3 to obtain percentage killing according to the formula: 100-(counts from the fabric of interest/average counts from control*100). (d-e) To examine the robustness of the fabrics, 10^4 CFU of *Klebsiella pneumoniae* ENT646 was added to (d) F#1 + yCu or (e) F#1 + aCu fabrics cumulatively at the indicated timepoints. All the assays were performed in triplicates and the values are expressed as mean ± S.D.

To determine the factors contributing to the mode of action of yCu and aCu and the possible difference in robustness, we examined bacterial morphology via SEM (Figure 4). A high dosage of 10^8 CFU *K. pneumoniae* and a prolonged duration of 1 hour was selected to increase the chances of visualizing the effects of the fabrics on bacteria. At this inoculating dose, both yCu- and aCu-coated fabrics exhibited approximately 47% to 62% killing (Figure SI6c). Indentations were observed on the bacterial surface after interaction of 10^8 CFU *K. pneumoniae* with both yCu- and aCu-coated fabrics F#1 for 1 hour (Figure 4b-d), suggesting bacterial cell surface structural damage.

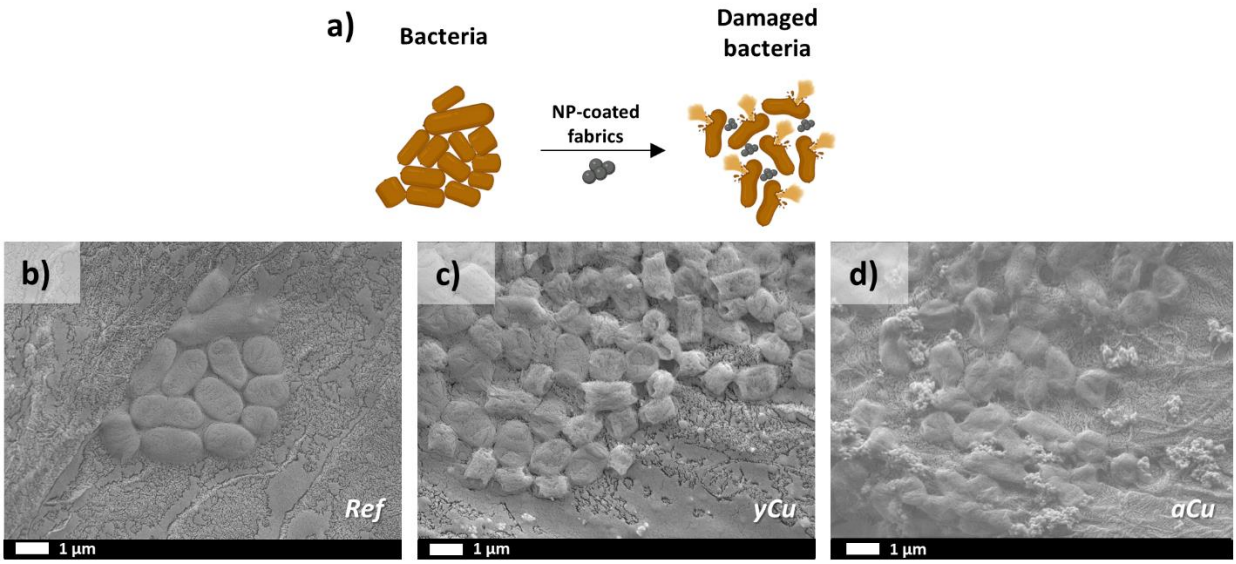

Figure 4. The surface of the yCu- and aCu-coated fabrics show bacterial damage. (a) Schematic illustration of the bacterial wall damage generated by copper nanoparticles in contact with bacteria. (b-d) SEM images of the fabrics after inoculation with Klebsiella pneumoniae ENT646. (b) Reference, (c) yCu-coated fabric, and (d) aCu-coated fabric.[50]

Additionally, bacterial DNA harvested after interaction of *K. pneumoniae* with yCu- and aCu-coated fabrics for 45 seconds and 1 hour resulted in a smeared band during gel electrophoresis, indicative of rapid DNA fragmentation within 45 seconds (Figure 5a). As oxidative stress can result in DNA fragmentation, we assessed the levels of 8-oxo-2'-deoxyguanosine (8OHdG), a marker of oxidative damage to deoxyguanosine (dG), after DNA contacts the copper-coated fabrics. Significantly higher levels of 8OHdG per 10,000 dG were detected after DNA interaction with both yCu- and aCu-coated fabrics compared to control fabric F#1 at 45 seconds and 1 hour, signifying that both copper NPs induce oxidative stress rapidly (Figure 5b). Between the two copper coated fabrics, aCu-coated fabrics resulted in greater oxidative damage of dG. This correlates with the lower atomic concentration of yCu (4.2%), which is approximately about half

of that of aCu (8.1%) on F#1 (Table SI1). These results indicate that both copper materials are capable of inducing bacterial structural damage and oxidative stress. However, additional antibacterial mechanisms may be involved as yCu displays equally high killing efficiencies and greater robustness despite lower nanoparticle surface coverage on fabric F#1 and the generation of oxidative damage.

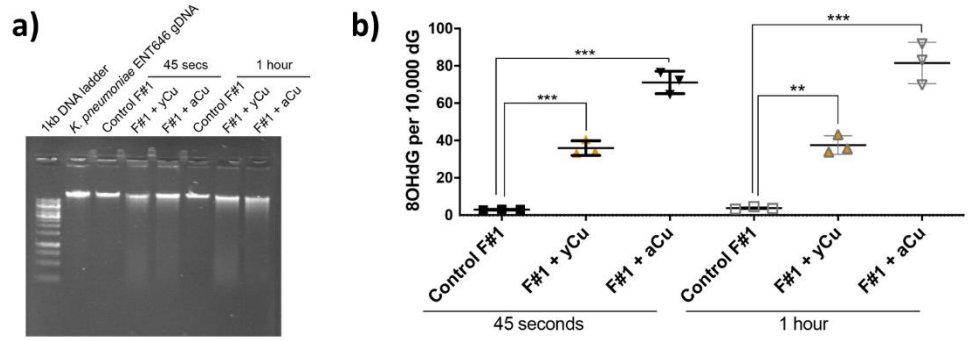

Figure 5. (a) Bacterial genomic DNA was assessed for DNA fragmentation after bacterial interaction with the indicated fabrics. Circular fabrics of 6 mm diameter were inoculated with 10^8 CFU bacteria for a duration of 45 seconds or 1 hour before extraction of DNA and examination of DNA fragmentation via gel electrophoresis. (b) Amount of oxidative damage marker 8-hydroxy-2' -deoxyguanosine (8OHdG) after DNA interaction with the fabrics. 50 µg of DNA was added to circular fabrics of 6 mm diameter for 45 seconds or 1 hour before DNA retrieval and examination via LC-MS. Levels of 8OHdG are expressed relative to 10,000dG. All the assays were performed in triplicates and the values are expressed as mean ± S.D. *P ≤ 0.05; **P ≤ 0.01; ***P ≤ 0.001; n.s., not significant.

CONCLUSIONS

We have demonstrated rapid high antibacterial efficacies of yCu and aCu copper-coated fabrics against Gram-positive bacteria *S. aureus* and Gram-negative bacteria *K. pneumoniae* and *P.*

aeruginosa. This reflects a broad spectrum of antibacterial activity where the copper-coated fabrics are likely effective against a wide variety of bacteria.

Based on DNA degradation and modification of deoxyguanosine as markers for oxidative damage, it is reasonable to propose that bacteria underwent rapid and significant oxidative damage within 45 seconds after contact with both yCu and aCu. This strongly indicates that ROS are generated by the copper-coated surfaces. Given that ROS also damage membrane lipids and proteins[59-60], the deformation and indentations observed on the bacterial surface after contact with yCu and aCu could potentially be a result of ROS production. The membrane deformation could also result from attractive electrostatic forces between the bacteria and the particles that potentiate the bacterium-nanoparticle interaction, hence resulting in increased membrane tension force. Additionally, non-translating NPs have been previously reported to induce mechanical damage via an increase in membrane tension resulting in membrane deformation, with larger clusters demonstrating more membrane stretching and disruption[20]. As discussed earlier, the presence of $Cu(OH)_2$ on the surface of the copper-coated fabrics is likely from a metastable phase, presumably due to significant water absorption on the oxide surface at high humidity. However, the aCu-coated fabric revealed a relatively high atomic concentration (68.2%) of Cu^{2+} before water treatment. These results suggest that the surface of the aCu-coated fabric had oxidized to Cu^{2+} easily after being coated which is somewhat expected because copper oxidizes to its most stable phase, CuO[61]. The cumulative addition of water showed a decrease in the hydroxide signal, probably being leached with the water, which compromised the killing efficiency. Notably, the yCu-coated fabric showed no effect on water addition, hence resulting in a stable and long-lasting killing efficacy. Moreover, the "contact-killing" effect of copper has been reported to depend on the uniformity of the coating layer and the number of NPs[62-65] on the surface of the fabric materials that makes contact with the

bacteria. In line with this, larger-sized yCu NP-coated fabrics were more robust in maintaining high levels of antimicrobial activity during repeated exposure to bacteria, despite lower surface coverage of yCu and lower induction of oxidative stress. It is probable that the larger particle size of yCu mechanically damages membranes with concomitant ROS production.

Overall, our results demonstrate that both copper-coated fabrics possess rapid high antimicrobial activity against a broad spectrum of bacteria. Multiple mechanisms including ROS generation and mechanical damage likely contribute to the efficiency and robustness of the copper-coated fabrics.

In summary, we have successfully fabricated copper-coated fabrics that show high killing efficiencies against Gram-negative and Gram-positive bacteria within 45 seconds. The copper NPs used in this study were thoroughly characterized in order to allow for the establishment of a correlation between concentration, particle size, surface charge and oxidation state on the antibacterial activity of the coatings. Herein, metallic copper and cuprous oxide NPs were spray-coated on fabrics with different chemical composition and structure. We have shown that features present in the fabric are capable of augmenting the amounts of NPs and hence resulting in an increased concentration of NPs. Significantly, both species of copper are capable of inducing bacterial structural damage and oxidative stress. Notably, Cu^+ (yCu) displays equally high killing efficiencies and greater robustness despite lower nanoparticle surface coverage and generation of oxidative stress, although they could also disrupt the cell membrane due to the stronger interactions with the bacteria in this study. Since both copper species have been prepared using the same deposition route and compared on the same platform, we can conclusively demonstrate that Cu^+ is most effective for robust biocidal coatings. The elucidation of the impact of the properties of different copper nanoparticles on the antibacterial activity undoubtedly contributes to paving the way for robust and effective antibacterial materials that can be coated on most surfaces.

ASSOCIATED CONTENT

Supporting Information. Photographs of the copper NP-coated fabrics (Figure SI1). XPS Cu 2p core-level spectrum corresponding to old yCu sample (Figure SI2). XRD patterns of aCu and yCu (Figure SI3). Survey-scan AES spectra of aCu and yCu (Figure SI4). SEM images and EDS maps of the fabrics coated with copper nanoparticle aggregates at low magnification (Figure SI5). Values of the atomic concentration (%) of copper obtained from the SEM-EDS maps (Table SI1). Bacterial counts obtained after various fabric interactions with carbapenem-resistant hypervirulent *Klebsiella pneumoniae* ENT646 (Figure SI6). Bacterial counts obtained after various fabric interactions with (a, e) carbapenem-resistant hypervirulent *Klebsiella pneumoniae* ENT646, (b, d) *Pseudomonas aeruginosa* PAO1 and (c) *Staphylococcus aureus* SA29213 (Figure SI7). XPS spectra from yCu- and aCu-coated fabrics before and after addition of deionized water (Figure SI8). Atomic concentrations of Cu, Cu_2O and $Cu(OH)_2$ determined using XPS Cu 2p binding energies for the yCu- and aCu-coated fabrics before and after addition of deionized water (Table SI2). (PDF).

AUTHOR INFORMATION

Corresponding Authors

Chee Lip Gan

School of Materials Science and Engineering, Nanyang Technological University, 50 Nanyang Avenue, Singapore 639798, Singapore; https://orcid.org/0000-0002-8420-3168; E-mail: clgan@ntu.edu.sg

Yunn-Hwen Gan

Infectious Diseases Translational Research Program, Department of Biochemistry, Yong Loo Lin School of Medicine, National University of Singapore, MD 7, 8 Medical Drive, Singapore 117596, Singapore; https://orcid.org/0000-0001-9881-6881; E-mail: bchganyh@nus.edu.sg

Yeng Ming Lam

School of Materials Science and Engineering, Nanyang Technological University, 50 Nanyang Avenue, Singapore 639798, Singapore; https://orcid.org/0000-0001-9390-8074; E-mail: ymlam@ntu.edu.sg

Authors

‡Rui A. Gonçalves

School of Materials Science and Engineering, Nanyang Technological University, 50 Nanyang Avenue, Singapore 639798, Singapore; https://orcid.org/0000-0003-4543-3945

‡Joanne W. K. Ku

Department of Biochemistry, National University of Singapore, MD 7, 8 Medical Drive, Singapore 117596, Singapore; https://orcid.org/0000-0002-0421-5741

Hao Zhang

School of Materials Science and Engineering, Nanyang Technological University, 50 Nanyang Avenue, Singapore 639798, Singapore; https://orcid.org/0000-0001-9853-944X

Teddy Salim

School of Materials Science and Engineering and Facility for Analysis Characterisation Testing and Simulation, Nanyang Technological University, 50 Nanyang Avenue, Singapore 639798, Singapore; https://orcid.org/0000-0002-8912-4717

Guodong Oo

Department of Biochemistry, National University of Singapore, MD 7, 8 Medical Drive, Singapore 117596, Singapore; https://orcid.org/0000-0001-5429-6933

Alfred A. Zinn

Kuprion, Inc., 4425 Fortran Dr., San Jose, CA 95134, USA

Chris Boothroyd

School of Materials Science and Engineering and Facility for Analysis Characterisation Testing and Simulation, Nanyang Technological University, 50 Nanyang Avenue, Singapore 639798, Singapore

Richard M. Y. Tang

Department of Biochemistry, National University of Singapore, MD 7, 8 Medical Drive, Singapore 117596, Singapore; https://orcid.org/0000-0001-8038-1189

Author Contributions

‡R.A.G., ‡J.W.K.K., G.C.L., Y.-H.G., and Y.-M.L. conceptualized this work. R.A.G., J.W.K.K., H.Z., T.S., G.O., and R.M.Y.T. designed the experiments, and processed and analyzed the data. The manuscript was written through contributions of all authors. All authors have given approval to the final version of the manuscript. ‡These authors contributed equally.

ACKNOWLEDGMENTS

The authors acknowledge useful discussions with Professor Barry Halliwell and the Facility for Analysis, Characterisation, Testing and Simulation, Nanyang Technological University, Singapore, for the use of their X-ray and electron microscopy facilities. We thank the

Carbapenemase-Producing Enterobacteriaceae in Singapore (CaPES) study group for the contribution of strain ENT636. This group included Benjamin Cherng, Deepak Rama Narayana, Douglas Chan Su Gin, De Partha Pratim, Hsu Li Yang, Indumathi Venkatachalam, Jeanette Teo, Michelle Ang, Kalisvar Marimuthu, Koh Tse Hsien, Nancy Tee, Nares Smitasin, Ng Oon Tek, Ooi Say Tat, Raymond Fong, Raymond Lin, Tzer Pin, Surinder Kaur Pada, Tan Thean Yen, and Thoon Koh Cheng. This research was supported by the Ministry of Education, Singapore, under its Academic Research Fund Tier 1 (Project No. RG98/19).

GRAPHICAL TABLE OF CONTENTS

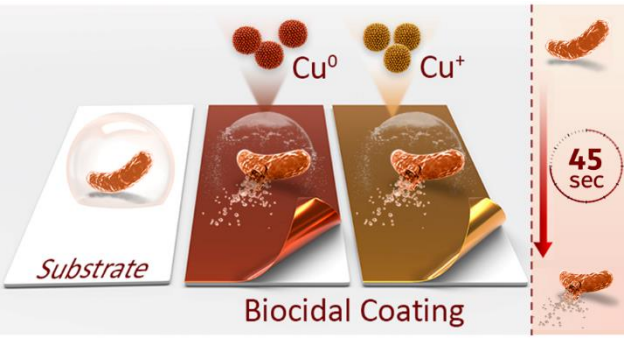

REFERENCES

(1) Inc., C. D. A. EPA Approves 73 Additional Copper Alloys as Antimicrobial. https://www.copper.org/about/pressreleases/2011/pr2011_Apr_22.html (accessed 15 December).

(2) Inc., C. D. A. U.S. EPA Approves Registration of Antimicrobial Copper Alloys. https://www.copper.org/about/pressreleases/2008/pr2008_Mar_25.html (accessed 15 December).

(3) Page, K.; Wilson, M.; Parkin, I. P. Antimicrobial surfaces and their potential in reducing the role of the inanimate environment in the incidence of hospital-acquired infections. *Journal of Materials Chemistry* **2009,** *19* (23), 3819-3831, DOI: 10.1039/B818698G.

(4) Wheeldon, L. J.; Worthington, T.; Lambert, P. A.; Hilton, A. C.; Lowden, C. J.; Elliott, T. S. J. Antimicrobial efficacy of copper surfaces against spores and vegetative cells of Clostridium difficile: the germination theory. *Journal of Antimicrobial Chemotherapy* **2008,** *62* (3), 522-525, DOI: 10.1093/jac/dkn219.

(5) Noyce, J. O.; Michels, H.; Keevil, C. W. Use of Copper Cast Alloys To Control Escherichia coli O157 Cross-Contamination during Food Processing. *Applied and Environmental Microbiology* **2006,** *72* (6), 4239-4244, DOI: 10.1128/aem.02532-05.

(6) Wilks, S. A.; Michels, H.; Keevil, C. W. The survival of Escherichia coli O157 on a range of metal surfaces. *International Journal of Food Microbiology* **2005,** *105* (3), 445-454, DOI: https://doi.org/10.1016/j.ijfoodmicro.2005.04.021.

(7) Imani, S. M.; Ladouceur, L.; Marshall, T.; Maclachlan, R.; Soleymani, L.; Didar, T. F. Antimicrobial Nanomaterials and Coatings: Current Mechanisms and Future Perspectives to Control the Spread of Viruses Including SARS-CoV-2. *ACS Nano* **2020,** *14* (10), 12341-12369, DOI: 10.1021/acsnano.0c05937.

(8) Li, X.; Bai, H.; Yang, Y.; Yoon, J.; Wang, S.; Zhang, X. Supramolecular Antibacterial Materials for Combatting Antibiotic Resistance. *Advanced Materials* **2019,** *31* (5), 1805092, DOI: https://doi.org/10.1002/adma.201805092.

(9) Vincent, M.; Duval, R. E.; Hartemann, P.; Engels-Deutsch, M. Contact killing and antimicrobial properties of copper. *Journal of Applied Microbiology* **2018,** *124* (5), 1032-1046, DOI: https://doi.org/10.1111/jam.13681.

(10) Wang, Z.; von dem Bussche, A.; Kabadi, P. K.; Kane, A. B.; Hurt, R. H. Biological and Environmental Transformations of Copper-Based Nanomaterials. *ACS Nano* **2013,** *7* (10), 8715-8727, DOI: 10.1021/nn403080y.

(11) Bezza, F. A.; Tichapondwa, S. M.; Chirwa, E. M. N. Fabrication of monodispersed copper oxide nanoparticles with potential application as antimicrobial agents. *Scientific Reports* **2020,** *10* (1), 16680, DOI: 10.1038/s41598-020-73497-z.

(12) Nan, L.; Liu, Y.; Lü, M.; Yang, K. Study on antibacterial mechanism of copper-bearing austenitic antibacterial stainless steel by atomic force microscopy. *Journal of Materials Science: Materials in Medicine* **2008,** *19* (9), 3057-3062, DOI: 10.1007/s10856-008-3444-z.

(13) Warnes, S. L.; Keevil, C. W. Lack of Involvement of Fenton Chemistry in Death of Methicillin-Resistant and Methicillin-Sensitive Strains of Staphylococcus aureus and Destruction of Their Genomes on Wet or Dry Copper Alloy Surfaces. *Applied and Environmental Microbiology* **2016,** *82* (7), 2132-2136, DOI: 10.1128/aem.03861-15.

(14) Sunada, K.; Minoshima, M.; Hashimoto, K. Highly efficient antiviral and antibacterial activities of solid-state cuprous compounds. *Journal of Hazardous Materials* **2012,** *235-236*, 265-270, DOI: https://doi.org/10.1016/j.jhazmat.2012.07.052.

(15) Cuypers, A.; Plusquin, M.; Remans, T.; Jozefczak, M.; Keunen, E.; Gielen, H.; Opdenakker, K.; Nair, A. R.; Munters, E.; Artois, T. J.; Nawrot, T.; Vangronsveld, J.; Smeets, K. Cadmium stress: an oxidative challenge. *BioMetals* **2010,** *23* (5), 927-940, DOI: 10.1007/s10534-010-9329-x.

(16) Collin, F. Chemical Basis of Reactive Oxygen Species Reactivity and Involvement in Neurodegenerative Diseases. *International Journal of Molecular Sciences* **2019,** *20* (10), 2407.

(17) Park, H.-J.; Nguyen, T. T. M.; Yoon, J.; Lee, C. Role of Reactive Oxygen Species in Escherichia coli Inactivation by Cupric Ion. *Environmental Science & Technology* **2012,** *46* (20), 11299-11304, DOI: 10.1021/es302379q.

(18) Warnes, S. L.; Caves, V.; Keevil, C. W. Mechanism of copper surface toxicity in Escherichia coli O157:H7 and Salmonella involves immediate membrane depolarization followed by slower rate of DNA destruction which differs from that observed for Gram-positive bacteria. *Environmental Microbiology* **2012,** *14* (7), 1730-1743, DOI: https://doi.org/10.1111/j.1462-2920.2011.02677.x.

(19) Minoshima, M.; Lu, Y.; Kimura, T.; Nakano, R.; Ishiguro, H.; Kubota, Y.; Hashimoto, K.; Sunada, K. Comparison of the antiviral effect of solid-state copper and silver compounds. *Journal of Hazardous Materials* **2016,** *312*, 1-7, DOI: https://doi.org/10.1016/j.jhazmat.2016.03.023.

(20) Linklater, D. P.; Baulin, V. A.; Le Guével, X.; Fleury, J.-B.; Hanssen, E.; Nguyen, T. H. P.; Juodkazis, S.; Bryant, G.; Crawford, R. J.; Stoodley, P.; Ivanova, E. P. Antibacterial Action of Nanoparticles by Lethal Stretching of Bacterial Cell Membranes. *Advanced Materials* **2020,** *32* (52), 2005679, DOI: https://doi.org/10.1002/adma.202005679.

(21) Quaranta, D.; Krans, T.; Santo, C. E.; Elowsky, C. G.; Domaille, D. W.; Chang, C. J.; Grass, G. Mechanisms of Contact-Mediated Killing of Yeast Cells on Dry Metallic Copper Surfaces. *Applied and Environmental Microbiology* **2011,** *77* (2), 416-426, DOI: 10.1128/aem.01704-10.

(22) Santo, C. E.; Taudte, N.; Nies, D. H.; Grass, G. Contribution of Copper Ion Resistance to Survival of Escherichia coli on Metallic Copper Surfaces. *Applied and Environmental Microbiology* **2008,** *74* (4), 977-986, DOI: 10.1128/aem.01938-07.

(23) Grass, G.; Rensing, C.; Solioz, M. Metallic Copper as an Antimicrobial Surface. *Applied and Environmental Microbiology* **2011,** *77* (5), 1541-1547, DOI: 10.1128/aem.02766-10.

(24) Linklater, D. P.; Baulin, V. A.; Juodkazis, S.; Crawford, R. J.; Stoodley, P.; Ivanova, E. P. Mechano-bactericidal actions of nanostructured surfaces. *Nature Reviews Microbiology* **2021,** *19* (1), 8-22, DOI: 10.1038/s41579-020-0414-z.

(25) Ghosh, S.; Mukherjee, S.; Patra, D.; Haldar, J. Polymeric Biomaterials for Prevention and Therapeutic Intervention of Microbial Infections. *Biomacromolecules* **2022,** *23* (3), 592-608, DOI: 10.1021/acs.biomac.1c01528.

(26) Klibanov, A. M. Permanently microbicidal materials coatings. *Journal of Materials Chemistry* **2007,** *17* (24), 2479-2482, DOI: 10.1039/B702079A.

(27) Sánchez-López, E.; Gomes, D.; Esteruelas, G.; Bonilla, L.; Lopez-Machado, A. L.; Galindo, R.; Cano, A.; Espina, M.; Ettcheto, M.; Camins, A.; Silva, A. M.; Durazzo, A.; Santini, A.; Garcia, M. L.; Souto, E. B. Metal-Based Nanoparticles as Antimicrobial Agents: An Overview. *Nanomaterials* **2020,** *10* (2), 292.

(28) Cheeseman, S.; Christofferson, A. J.; Kariuki, R.; Cozzolino, D.; Daeneke, T.; Crawford, R. J.; Truong, V. K.; Chapman, J.; Elbourne, A. Antimicrobial Metal Nanomaterials: From Passive

to Stimuli-Activated Applications. *Advanced Science* **2020,** *7* (10), 1902913, DOI: https://doi.org/10.1002/advs.201902913.

(29) Kadiyala, U.; Kotov, A. N.; VanEpps, S. J. Antibacterial Metal Oxide Nanoparticles: Challenges in Interpreting the Literature. *Current Pharmaceutical Design* **2018,** *24* (8), 896-903, DOI: http://dx.doi.org/10.2174/1381612824666180219130659.

(30) Gold, K.; Slay, B.; Knackstedt, M.; Gaharwar, A. K. Antimicrobial Activity of Metal and Metal-Oxide Based Nanoparticles. *Advanced Therapeutics* **2018,** *1* (3), 1700033, DOI: https://doi.org/10.1002/adtp.201700033.

(31) Tripathi, N.; Goshisht, M. K. Recent Advances and Mechanistic Insights into Antibacterial Activity, Antibiofilm Activity, and Cytotoxicity of Silver Nanoparticles. *ACS Applied Bio Materials* **2022,** *5* (4), 1391-1463, DOI: 10.1021/acsabm.2c00014.

(32) Meghana, S.; Kabra, P.; Chakraborty, S.; Padmavathy, N. Understanding the pathway of antibacterial activity of copper oxide nanoparticles. *RSC Advances* **2015,** *5* (16), 12293-12299, DOI: 10.1039/C4RA12163E.

(33) Hosseini, M.; Chin, A. W. H.; Behzadinasab, S.; Poon, L. L. M.; Ducker, W. A. Cupric Oxide Coating That Rapidly Reduces Infection by SARS-CoV-2 via Solids. *ACS Appl. Mater. Interfaces* **2021,** *13* (5), 5919-5928, DOI: 10.1021/acsami.0c19465.

(34) Behzadinasab, S.; Chin, A.; Hosseini, M.; Poon, L.; Ducker, W. A. A Surface Coating that Rapidly Inactivates SARS-CoV-2. *ACS Appl. Mater. Interfaces* **2020,** *12* (31), 34723-34727, DOI: 10.1021/acsami.0c11425.

(35) Ermini, M. L.; Voliani, V. Antimicrobial Nano-Agents: The Copper Age. *ACS Nano* **2021,** *15* (4), 6008-6029, DOI: 10.1021/acsnano.0c10756.

(36) Behzadinasab, S.; Williams, M. D.; Hosseini, M.; Poon, L. L. M.; Chin, A. W. H.; Falkinham, J. O.; Ducker, W. A. Transparent and Sprayable Surface Coatings that Kill Drug-Resistant Bacteria Within Minutes and Inactivate SARS-CoV-2 Virus. *ACS Appl. Mater. Interfaces* **2021,** *13* (46), 54706-54714, DOI: 10.1021/acsami.1c15505.

(37) Kwong, L. H.; Wilson, R.; Kumar, S.; Crider, Y. S.; Reyes Sanchez, Y.; Rempel, D.; Pillarisetti, A. Review of the Breathability and Filtration Efficiency of Common Household Materials for Face Masks. *ACS Nano* **2021,** *15* (4), 5904-5924, DOI: 10.1021/acsnano.0c10146.

(38) Zhao, M.; Liao, L.; Xiao, W.; Yu, X.; Wang, H.; Wang, Q.; Lin, Y. L.; Kilinc-Balci, F. S.; Price, A.; Chu, L.; Chu, M. C.; Chu, S.; Cui, Y. Household Materials Selection for Homemade Cloth Face Coverings and Their Filtration Efficiency Enhancement with Triboelectric Charging. *Nano Letters* **2020,** *20* (7), 5544-5552, DOI: 10.1021/acs.nanolett.0c02211.

(39) Chen, Y.; Marimuthu, K.; Teo, J.; Venkatachalam, I.; Cherng, B. P. Z.; De Wang, L.; Prakki, S. R. S.; Xu, W.; Tan, Y. H.; Nguyen, L. C.; Koh, T. H.; Ng, O. T.; Gan, Y. H. Acquisition of Plasmid with Carbapenem-Resistance Gene blaKPC2 in Hypervirulent Klebsiella pneumoniae, Singapore. *Emerg Infect Dis* **2020,** *26* (3), 549-559, DOI: 10.3201/eid2603.191230.

(40) Weaver, L.; Noyce, J. O.; Michels, H. T.; Keevil, C. W. Potential action of copper surfaces on meticillin-resistant Staphylococcus aureus. *J Appl Microbiol* **2010,** *109* (6), 2200-5, DOI: 10.1111/j.1365-2672.2010.04852.x.

(41) Ingle, A. P.; Duran, N.; Rai, M. Bioactivity, mechanism of action, and cytotoxicity of copper-based nanoparticles: A review. *Applied Microbiology and Biotechnology* **2014,** *98* (3), 1001-1009, DOI: 10.1007/s00253-013-5422-8.

(42) Biesinger, M. C. Advanced analysis of copper X-ray photoelectron spectra. *Surface and Interface Analysis* **2017,** *49* (13), 1325-1334, DOI: https://doi.org/10.1002/sia.6239.

(43) Biesinger, M. C.; Lau, L. W. M.; Gerson, A. R.; Smart, R. S. C. Resolving surface chemical states in XPS analysis of first row transition metals, oxides and hydroxides: Sc, Ti, V, Cu and Zn. *Applied Surface Science* **2010,** *257* (3), 887-898, DOI: https://doi.org/10.1016/j.apsusc.2010.07.086.

(44) Platzman, I.; Brener, R.; Haick, H.; Tannenbaum, R. Oxidation of Polycrystalline Copper Thin Films at Ambient Conditions. *The Journal of Physical Chemistry C* **2008,** *112* (4), 1101-1108, DOI: 10.1021/jp076981k.

(45) Leapman, R. D.; Grunes, L. A.; Fejes, P. L. Study of the L23 edges in the 3d transition metals and their oxides by electron-energy-loss spectroscopy with comparisons to theory. *Physical Review B* **1982,** *26* (2), 614-635, DOI: 10.1103/PhysRevB.26.614.

(46) Wang, Y.; Lany, S.; Ghanbaja, J.; Fagot-Revurat, Y.; Chen, Y. P.; Soldera, F.; Horwat, D.; Mücklich, F.; Pierson, J. F. Electronic structures of Cu2O, Cu4O3, and CuO: A joint experimental and theoretical study. *Physical Review B* **2016,** *94* (24), 245418, DOI: 10.1103/PhysRevB.94.245418.

(47) Laffont, L.; Wu, M. Y.; Chevallier, F.; Poizot, P.; Morcrette, M.; Tarascon, J. M. High resolution EELS of Cu–V oxides: Application to batteries materials. *Micron* **2006,** *37* (5), 459-464, DOI: https://doi.org/10.1016/j.micron.2005.11.007.

(48) Zhu, P.; Masuda, Y.; Koumoto, K. Seedless micropatterning of copper by electroless deposition on self-assembled monolayers. *Journal of Materials Chemistry* **2004,** *14* (6), 976-981, DOI: 10.1039/B311061C.

(49) Mazurkow, J. M.; Yüzbasi, N. S.; Domagala, K. W.; Pfeiffer, S.; Kata, D.; Graule, T. Nano-Sized Copper (Oxide) on Alumina Granules for Water Filtration: Effect of Copper Oxidation State

on Virus Removal Performance. *Environmental Science & Technology* **2020,** *54* (2), 1214-1222, DOI: 10.1021/acs.est.9b05211.

(50) Lam, Y. M.; Goncalves Cardoso, R. A.; Salim, T. Copper nanoparticle formulation to promote rapid pathogen inactivation. WO/2022/098299, 2022.

(51) Chen, Y.; Marimuthu, K.; Teo, J.; Venkatachalam, I.; Cherng, B. P. Z.; De Wang, L.; Prakki, S. R. S.; Xu, W.; Tan, Y. H.; Nguyen, L. C.; Koh, T. H.; Ng, O. T.; Gan, Y.-H. Acquisition of Plasmid with Carbapenem-Resistance Gene blaKPC2 in Hypervirulent Klebsiella pneumoniae, Singapore. *Emerging infectious diseases* **2020,** *26* (3), 549-559, DOI: 10.3201/eid2603.191230.

(52) Brown, S.; Santa Maria, J. P., Jr.; Walker, S. Wall teichoic acids of gram-positive bacteria. *Annu Rev Microbiol* **2013,** *67*, 313-36, DOI: 10.1146/annurev-micro-092412-155620.

(53) Simpson, B. W.; Trent, M. S. Pushing the envelope: LPS modifications and their consequences. *Nat Rev Microbiol* **2019,** *17* (7), 403-416, DOI: 10.1038/s41579-019-0201-x.

(54) Clements, A.; Gaboriaud, F.; Duval, J. F.; Farn, J. L.; Jenney, A. W.; Lithgow, T.; Wijburg, O. L.; Hartland, E. L.; Strugnell, R. A. The major surface-associated saccharides of Klebsiella pneumoniae contribute to host cell association. *PLoS One* **2008,** *3* (11), e3817, DOI: 10.1371/journal.pone.0003817.

(55) Shephard, J.; McQuillan, A. J.; Bremer, P. J. Mechanisms of Cation Exchange by Pseudomonas aeruginosa PAO1 and PAO1 wbpL, a Strain with a Truncated Lipopolysaccharide. *Appl Environ Microbiol* **2008,** *74* (22), 6980-6, DOI: 10.1128/AEM.01117-08.

(56) Fernandez-Grajera, M.; Pacha-Olivenza, M. A.; Gallardo-Moreno, A. M.; Gonzalez-Martin, M. L.; Perez-Giraldo, C.; Fernandez-Calderon, M. C. Modification of physico-chemical surface properties and growth of Staphylococcus aureus under hyperglycemia and ketoacidosis conditions. *Colloids Surf B Biointerfaces* **2021,** *209* (Pt 1), 112137, DOI: 10.1016/j.colsurfb.2021.112137.

(57) Shireen, T.; Singh, M.; Das, T.; Mukhopadhyay, K. Differential adaptive responses of Staphylococcus aureus to in vitro selection with different antimicrobial peptides. *Antimicrob Agents Chemother* **2013,** *57* (10), 5134-7, DOI: 10.1128/AAC.00780-13.

(58) Opal, S. M. Significance of sialic acid in Klebsiella pneumoniae K1 capsules. *Virulence* **2014,** *5* (6), 648-9, DOI: 10.4161/viru.34349.

(59) Joshi, S. G.; Cooper, M.; Yost, A.; Paff, M.; Ercan, U. K.; Fridman, G.; Friedman, G.; Fridman, A.; Brooks, A. D. Nonthermal Dielectric-Barrier Discharge Plasma-Induced Inactivation Involves Oxidative DNA Damage and Membrane Lipid Peroxidation in Escherichia coli. *Antimicrobial Agents and Chemotherapy* **2011,** *55* (3), 1053-1062, DOI: 10.1128/aac.01002-10.

(60) Tamarit, J.; Cabiscol, E.; Ros, J. Identification of the major oxidatively damaged proteins in Escherichia coli cells exposed to oxidative stress. *J Biol Chem* **1998,** *273* (5), 3027-3032, DOI: 10.1074/jbc.273.5.3027.

(61) Bard, A. J., Parsons, R., & Jordan, J. *Standard Potentials in Aqueous Solution*, CRC Press: 1985.

(62) Zhu, L.; Elguindi, J.; Rensing, C.; Ravishankar, S. Antimicrobial activity of different copper alloy surfaces against copper resistant and sensitive Salmonella enterica. *Food Microbiology* **2012,** *30* (1), 303-310, DOI: https://doi.org/10.1016/j.fm.2011.12.001.

(63) Souli, M.; Galani, I.; Plachouras, D.; Panagea, T.; Armaganidis, A.; Petrikkos, G.; Giamarellou, H. Antimicrobial activity of copper surfaces against carbapenemase-producing contemporary Gram-negative clinical isolates. *Journal of Antimicrobial Chemotherapy* **2012,** *68* (4), 852-857, DOI: 10.1093/jac/dks473.

(64) Elguindi, J.; Wagner, J.; Rensing, C. Genes involved in copper resistance influence survival of Pseudomonas aeruginosa on copper surfaces. *Journal of Applied Microbiology* **2009,** *106* (5), 1448-1455, DOI: https://doi.org/10.1111/j.1365-2672.2009.04148.x.

(65) Mehtar, S.; Wiid, I.; Todorov, S. D. The antimicrobial activity of copper and copper alloys against nosocomial pathogens and Mycobacterium tuberculosis isolated from healthcare facilities in the Western Cape: an in-vitro study. *Journal of Hospital Infection* **2008,** *68* (1), 45-51, DOI: 10.1016/j.jhin.2007.10.009.